

This document is intended for publication in a journal, and is made available on the understanding that extracts or references will not be published prior to publication of the original, without the consent of the authors.

CLM - P 430



UKAEA RESEARCH GROUP

Preprint



MAGNETOHYDRODYNAMIC PRESSURE DROP IN DUCTED TWO-PHASE FLOWS

R G OWEN
J C R HUNT
J G COLLIER

CULHAM LABORATORY
Abingdon Oxfordshire

1975

This document is intended for publication in a journal or at a conference and is made available on the understanding that extracts or references will not be published prior to publication of the original, without the consent of the authors.

Enquiries about copyright and reproduction should be addressed to the Librarian, UKAEA, Culham Laboratory, Abingdon, Oxfordshire, England

MAGNETOHYDRODYNAMIC PRESSURE DROP IN DUCTED
TWO-PHASE FLOWS

R.G. Owen†, J.C.R. Hunt* and J.G. Collier†
Culham Laboratory, Abingdon, Oxon, OX14 3DB, UK
(Euratom/UKAEA Fusion Association)

ABSTRACT

Two models are presented for predicting magnetohydrodynamic pressure drop in two-phase gas-liquid flows of conducting fluids for large values of Hartmann number. The first of these models treats the gas-liquid mixture as a single homogeneous pseudofluid with averaged mixture properties. The second model assumes that the flow pattern is one where the liquid is displaced to the duct walls as a liquid film and the gas flows in the central core.

It is shown that the two models do not differ significantly in their predictions of overall pressure drop for vaporising two-phase flow of potassium.

† AERE Harwell

* University of Cambridge

(Submitted for publication in Int. J. Two-Phase Flow)

June 1975

CONTENTS

	Page
1. INTRODUCTION	1
2. FLOW MODELS -	1
2.1 Homogeneous Model	1
2.2 Two-phase MHD Film Flow	2
2.3 Solution Procedure	3
3. DISCUSSION OF RESULTS	3
4. CONCLUSIONS	4
REFERENCES	4
NOMENCLATURE	5

1. INTRODUCTION

During the last 5 years, a great deal of effort has been expended both in analysing magneto-hydrodynamic single phase duct flows and in experimentally verifying the results of these analyses^(1,2). Very little attention has, however, been directed to the prediction of gas-liquid two-phase magneto-hydrodynamics. This is not surprising - the highly empirical nature of two-phase flow analyses gives little hope for the prediction of two phase MHD flows without extensive experimental data, which is not currently available. One limiting case is, however, amenable to study, that of two-phase flow in which the Hartmann number for the liquid phase is very large (electro-magnetic stresses dominate the viscous stresses).

This limiting case, moreover, has practical significance. For example, in a steady state deuterium-tritium fusion reactor, a high temperature reacting plasma is magnetically confined and produces the majority of its reaction energy as 14 MeV neutrons. These neutrons are thermalised in a lithium-bearing blanket from which heat has to be recovered at a sufficiently high temperature for the efficient generation of electrical power. One proposed method for cooling this lithium blanket is to employ potassium as a heat transfer fluid. Liquid potassium is pumped through the toroidal confining magnetic field into the lithium blanket region in which it is boiled and from which it emerges as a vapour which is passed through a turbine or heat exchanger. The computation of pressure losses in such a primary coolant circuit requires knowledge of the pressure drop occurring in the MHD two-phase boiling region.

In this paper, two simple models are presented for the computation of pressure drop in MHD two-phase flow at high Hartmann numbers. A comparison is made between the predictions of the two models for the case of potassium boiling at constant heat flux in a uniform duct.

2. FLOW MODELS

2.1 Homogeneous Model

This model assumes that the two-phase flow may be adequately represented by a single-phase flow having pseudo-properties calculated by suitably weighting the properties of the individual phases. An equivalent two-phase electrical conductivity has been derived by Hall-Taylor⁽³⁾ as

$$\sigma_{TP} = \sigma_L / (1 + 1300X) \quad 2.1.1$$

based on experimental data for air-water and potassium. This form of correlation* implies that the two-phase electrical conductivity is independent of the density ratio of the phases. Strictly, this cannot be true, but though there is probably a weak dependence of σ_{TP} on the density ratio ρ_L/ρ_G , use of equation 2.1.1 should be reasonably accurate for most systems. An equivalent two-phase volumetric flow-rate is defined

$$Q_{TP} = Q \left[1 + X \left\{ \frac{V_G - V_L}{V_L} \right\} \right] \quad 2.1.2$$

The wall conductance ratio for two-phase flow may be defined:

$$\phi_{TP} = \left\{ \frac{\sigma_{wt}}{\sigma_{TPr}} \right\} = \theta (1 + 1300X) \quad 2.1.3$$

provided there is no contact resistance between the fluid and the wall. An equivalent two-phase Hartmann number is given by

$$M_{TP} = rB (\sigma_{TP}/\nu_{TP})^{1/2} \quad 2.1.4$$

If ν_{TP} is equated with the liquid phase kinematic viscosity, the equivalent two-phase Hartmann number becomes

$$M_{TP} = M_L / (1 + 1300X)^{1/2} \quad 2.1.5$$

The homogeneous model for two-phase pressure drop at high Hartmann numbers yields⁽⁵⁾

$$\left. \frac{\partial P}{\partial z} \right|_{TP} = \frac{-Q_{TP} \sigma_{TP} B^2}{A} \left\{ \frac{\phi_{TP}}{1 + \phi_{TP}} \right\} \quad 2.1.6$$

For mass qualities of $0.05 < X < 1$, $\phi_{TP} \gg 1$ then

$$\left. \frac{\partial P}{\partial z} \right|_{TP} = \frac{Q_{TP} \sigma_{TP} B^2}{A} = \left. \frac{\partial P}{\partial z} \right|_L \frac{\left[1 + X \left\{ \frac{V_G - V_L}{V_L} \right\} \right]}{1 + 1300X} \quad 2.1.7$$

Equation 2.1.7 directly relates the two-phase pressure gradient to the pressure gradient which would exist if liquid only flowed through the duct at the same mass velocity as the two-phase mixture. The latter is readily computed from well-established equations⁽⁵⁾.

A more sophisticated approach is to specify a "flow pattern" within the framework of an idealised representation. It therefore appears necessary to direct attention to a flow pattern in which there is

* Alternative forms of correlation express the two-phase electrical conductivity as a function of void fraction⁽⁴⁾.

a liquid continuum adjacent to the duct wall while in the centre of the duct there is a vapour continuum. Such a flow is commonly termed "annular flow"⁽⁶⁾, and typically occurs over a substantial portion of the boiling region in a duct. In this report, the terms "annular flow" and "film flow" will denote a flow in which the liquid is displaced to the heated walls and the vapour is a continuum in the central core of the duct.

2.2 Two-phase "annular" MHD flow

Consider a rectangular duct with an applied transverse uniform magnetic field (Fig 1). A conducting fluid of electrical conductivity " σ " flows through the duct and is initially all liquid. To the top and bottom faces of the duct is applied a constant heat flux " h ". Attention is focussed on the two-phase region. The first bubbles of vapour formed at the duct surface will tend to produce a bubbly flow, but an "annular" flow regime should be quickly established. The flow is characterised by gradual thinning of the liquid film and increasing vapour flow. The liquid phase experiences a large MHD force opposing its motion while the vapour flow exerts a large interfacial drag force on the liquid film. To make analysis tractable, the "annular" flow condition will be assumed to commence at the inception of vapour formation. For large values of Hartmann number (i.e. provided $fB (\sigma/\nu)^{1/2} \geq 130 fU_G/\nu$) the large magnetic damping forces in the liquid phase will prevent the onset of turbulence in the liquid film. Wave formation at the vapour-liquid interface may be suppressed, greatly decreasing phase interaction and entrainment. The simplifying assumption is made that the vapour liquid interface is smooth and that there is no entrainment from the liquid film to the vapour core.

The effect of the magnetic field on the two-phase flow may now be considered. The motion of the conducting fluid induces an electric field $\underline{U} \times \underline{B}$ in the liquid phase, where \underline{U} is the velocity and \underline{B} the local magnetic flux density. Typical current paths for two-phase "annular" flow in a rectangular duct are shown in Fig 2. If the walls of the duct are electrical insulators the currents generated in the bulk of the liquid film return through the film itself. If the duct walls are highly conducting then the currents return through the duct walls. The electric currents induce their own magnetic field which is mainly directed along the duct because the currents flow in transverse loops. The ratio of this induced field to the imposed magnetic field is known as the Magnetic Reynolds number and is

usually small.

Consider the flow at a cross-section such as A-A in Fig 1.

Conservation of mass in the duct requires

$$\rho_G \int_f^a U_G dy + \rho_L \int_o^f U_L dy = \frac{\dot{m}}{4b} \quad 2.2.1$$

If the fluid properties and saturation temperature are only slowly varying along the channel, an elemental heat balance yields

$$h = \lambda \rho_L \frac{d}{dz} \left\{ \int_o^f U_L dy \right\} \quad 2.2.2.$$

which reduces to

$$h = -\lambda \rho_L \left\{ U_L \left|_{y=f} \frac{df}{dz} + \int_o^f \frac{\partial U_L}{\partial z} dy \right. \right\} \quad 2.2.3$$

If the liquid flow is assumed to be laminar, an elemental force balance for the film may be written as

$$-\frac{\partial p}{\partial z} + \sigma E_x B - \sigma U_L B^2 + \mu_L \frac{\partial^2 U_L}{\partial y^2} = 0 \quad 2.2.4$$

For the gas phase, provided acceleration effects are not significant, a force balance exists between the pressure gradient and the shear force at the vapour liquid interface

$$-\frac{\partial p}{\partial z} = C \cdot \rho_G \bar{U}_G^2 / (a - f) \quad 2.2.5$$

where "C" is a frictional coefficient, evaluated assuming that the vapour flows through an essentially stationary duct. For the large gas to liquid relative velocities which would be characteristic of these MHD flows, this approximation should be accurate. The frictional coefficient is estimated from the results for smooth-walled tubes. (The liquid surface may have waves on it which would increase the drag coefficient)

$$C = 16/Re_G ; 0 < Re_G \leq 2000 \quad 2.2.6(a)$$

$$C = \frac{1}{4} \left\{ 0.86859 \ln [Re_G / 1.964 \ln Re_G] - 3.8215 \right\}^{-2} \quad \text{for } Re_G > 2000 \quad 2.2.6(b)$$

Induced eddy currents are assumed to circulate in the x-y plane (this is only true provided u_L and f vary slowly along the duct) thus, if the duct walls are thin, of thickness " t " and conducting with electrical conductivity " σ_w "

$$\sigma \int_o^f (E_x - U_L B) dy = -E_x \sigma_w t \quad 2.2.7$$

but

$$\frac{\partial E_x}{\partial y} = 0 \quad 2.2.8$$

Hence

$$E_x = B \int_0^f U_L dy / f(1 + \phi_f) \quad 2.2.9$$

where ϕ_f is the relative conductance of the duct wall to the film. From equation 2.2.9 it may be observed that $\frac{\partial E_x}{\partial z} \neq 0$ and since $\frac{\partial E_z}{\partial x} = \frac{\partial E_x}{\partial z}$, a

current j_z is induced in the film.

This implies that the pressure within the duct varies with the x-coordinate so that the thickness of the liquid film varies across the duct. This effect is small, however, because change in E_x takes place over a distance large compared with "a" or "b".

Equations 2.2.1, 2.2.2, 2.2.4, 2.2.5 and 2.2.9 comprise a set of five equations for the parameters U_L , \dot{m}_G , f , E_x , $\frac{\partial P}{\partial z}$. The following boundary con-

ditions apply. Liquid film velocity is zero at the solid surfaces hence

$$y = \pm a ; U_L = 0 \quad 2.2.10(a)$$

There is no discontinuity in the velocity profile at the gas/vapour interface (a discontinuity would imply a locally infinite shear stress)

$$y = \pm(a - f) ; U_L = U_G \quad 2.2.10(b)$$

The shear stress exerted by the liquid on the vapour phase at the interface must equal the shear stress exerted by the vapour flow on the liquid film

$$\mu_L \left. \frac{\partial U_L}{\partial y} \right|_I = \mu_G \left. \frac{\partial U_G}{\partial y} \right|_I = \tau_I \quad 2.2.10(c)$$

The film flow of liquid at any section must equal the total liquid flow at inlet, less the quantity vaporised. Thus

$$U_L f = - \int_0^z \frac{h}{\lambda \rho_L} dz + a U_L \Big|_{z=0} \quad 2.2.10(d)$$

2.3 Solution Procedure

For large liquid film Hartmann numbers, viscous effects in the film may be neglected so that the velocity in the film " U_L " will be independent of "y". In fact, as illustrated in Fig 3, there are thin Hartmann layers both on the wall and on the liquid-air interface. These Hartmann layers have a characteristic thickness of (f/M) where f is the liquid film thickness and M is the Hartmann number.

Combining equations 2.2.4 and 2.2.9 yields

$$-\frac{\partial P}{\partial z} - \sigma U_L B^2 \left\{ 1 + \frac{1}{1 + \phi_f} \right\} = 0 \quad 2.3.1$$

Similarly, equations 2.2.1 and 2.2.5 may be combined to give

$$U_L = \left\{ \frac{\dot{m}}{4b} - \frac{\rho_G^{1/2} (a-f)^{3/2} \left[-\frac{\partial P}{\partial z} \right]^{1/2}}{c^{1/2}} \right\} / \rho_L f \quad 2.3.2$$

Equations 2.3.1, 2.3.2 and 2.2.10(c) are solved iteratively using a Newton-Raphson procedure for specified values of m , h , λ , a , b , B , σ_w , t , σ , ρ_G and ρ_L .

3. DISCUSSION OF RESULTS

Sample results are presented for the boiling of potassium in a rectangular duct.

Figs 4, 5 and 6 present the variation of U_L , f , E_x , $\frac{\partial P}{\partial z}$ and \dot{m}_G with axial position for values of

input parameters given below in table 1. It may be observed that the film flow model predicts that the liquid film remains appreciably thick for a considerable region and then rapidly thins. When the liquid film becomes thin, viscous and turbulent effects dominate, and the flow becomes like the usual viscous dominated two-phase annular flow.

For thick films, MHD film flow behaves differently from the more common viscous film flow. In the latter case the film is reduced both by evaporation and by axially increasing interfacial shear forces, whereas, in the former case, film thickness is determined by a local balance between MHD holdup and evaporation effects.

Figs 4, 5 and 6 show that the MHD film model predicts that the pressure gradient decreases in a near linear manner to the single phase value at the point of dryout. At a constant applied heating rate, the mass flow of vapour increases linearly. The slightly anomalous behaviour of the film flow model at very low qualities is attributable to the laminar-turbulent transition in the gas-phase - in reality the flow pattern would be bubbly at such low qualities.

Comparisons have been made between the pressure drops predicted by the two models for boiling flow of potassium in a rectangular duct. Graphs 7, 8, 9 and 10 show the effect of various parameters on predicted pressure-drop in a two-phase boiling potassium flow. From these figures, it may be observed that

TABLE 1

Input parameters for two-phase boiling potassium

Parameter	Numerical Value	Parameter	Numerical Value
\dot{m}	0.00127 (kg/s)	t	0.1×10^{-2} (m)
h	2×10^4 (W/m ²)	ρ_G	0.53 (kg/m ³)
λ	1.87×10^6 (J/kg)	ρ_L	662.2 (kg/m ³)
a	1×10^{-2} (m)	μ_G	2.49×10^{-5} (kg/ms)
b	2×10^{-2} (m)	σ	1.35×10^6 (mho/m)
B	5.0 (tesla)	$(V_G - V_L)/V_L$	1300 (-)
σ_w	5×10^6 (mho/m)	μ_L	1.29×10^{-4} (kg/ms)

for a given duct

1. The discrepancy between predicted pressure gradients remains approximately constant as the heat flux increases.
2. As the mass flow is decreased, the discrepancy between the predicted pressure gradients tends to increase.
3. The disagreement in predicted pressure gradients between the homogeneous model and the film model is, to first approximation, independent of magnetic field intensity.
4. The discrepancy between predicted pressure gradients tends to increase as the wall thickness increases.

These observations indicate the effect of different parameters on the pressure gradient predicted by two different models of two-phase flow in a duct at high Hartmann numbers. The model in which a specific flow pattern is assumed (the film flow pattern, in this case) generally predicts lower pressure gradients in boiling potassium than does the model in which the phases are considered as a homogeneous mixture.

4. CONCLUSIONS

A simple homogeneous model of two-phase MHD pressure drop at large Hartmann numbers is presented and compared with the predictions of a more sophisticated film flow model. For once-through, induct vaporisation of potassium the two models usually predict overall two-phase pressure gradients which agree within 50% although, in certain cases, discrepancies up to 100% are observed.

References

1. Hunt, J.C.R. and Shercliff, J.A. "High

Hartmann number magnetohydrodynamics", *Ann. Rev. Fluid Mechanics* 3, 37, (1971).

2. Branover, G.G. and Tsinober, A.B. "Magneto-hydrodynamics of incompressible fluids" (in Russian), Moscow (1970).
3. Hall-Taylor, N. "An assessment of liquid metal MHD systems for power generation", private communication (1967).
4. Fujii-e, Y. and Suita, T. "Blanket cooling with liquid metal as working fluid", IAEA Workshop on Fusion Reactor Design Problems, Culham Laboratory UK, 29 January - 15 February (1974).
5. Hunt, J.C.R. and Hancox, R. "The use of liquid lithium as coolant in a toroidal fusion reactor - Part I - calculation of pumping power", Culham Laboratory Report CLM-R115 (1971).
6. Hewitt, G.F. and Hall-Taylor, N. "Annular two-phase flow". Pergamon press (1970).

Nomenclature

A	duct cross-sectional area	(m ²)
a,b	half-widths of duct	(m)
B	magnetic field intensity transverse to flow	(tesla)
C	coefficient of friction	(-)
E	electric field	(V/m)
f	liquid film thickness	(m)
h	applied heat flux	(W/m ²)
j	current	(amperes)
M	Hartmann number of liquid film - $Bf (\sigma_L/\nu_L)^{\frac{1}{2}}$	(-)
m	total mass flow rate in the duct	(kg/s)
P	pressure	(N/m ²)
Q	volumetric flow rate	(m ³ /s)
r	radius or hydraulic radius	(m)
Re	Reynolds number	(-)
t	thickness	(m)
U	velocity	(m/s)
\bar{U}_G	average gas phase velocity	(m/s)
V	specific volume	(m ³ /kg)
x	co-ordinate transverse to the applied magnetic field	(m)
X	mass quality	(-)
y	co-ordinate aligned with the applied magnetic field	(m)
z	axial distance	(m)
σ	electrical conductivity	(mho/m)
ϕ	wall conductance ratio	(-)
ϕ_f	relative conductance of the duct walls to the liquid film	(-)
μ	absolute viscosity	(kg/ms)
ν	kinematic viscosity	(m ² /s)
ρ	density	(kg/m ³)
λ	latent heat of liquid/unit mass	(J/kg)
τ	shear stress	(N/m ²)

Subscripts

TP	two-phase
L	liquid-phase
G	vapour-phase
W	duct wall
I	interface of vapour-liquid

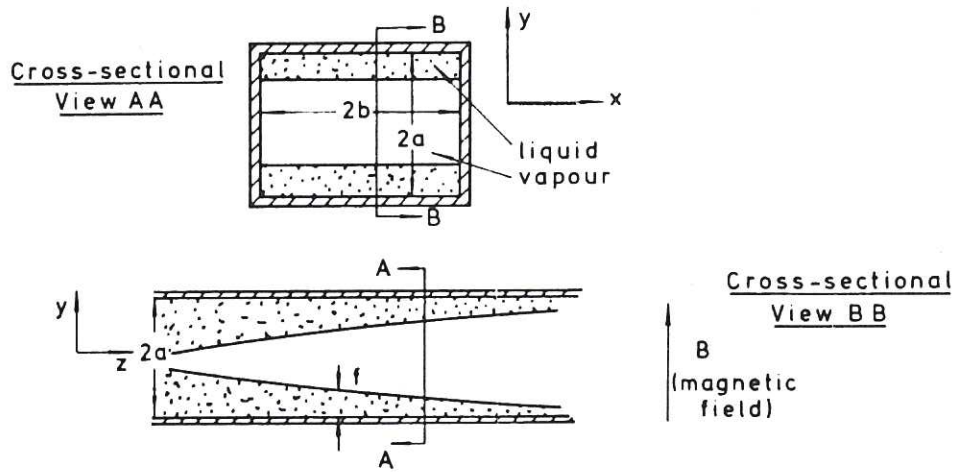


FIG.1. ASSUMED FLOW PATTERN FOR THE FILM FLOW MODEL.

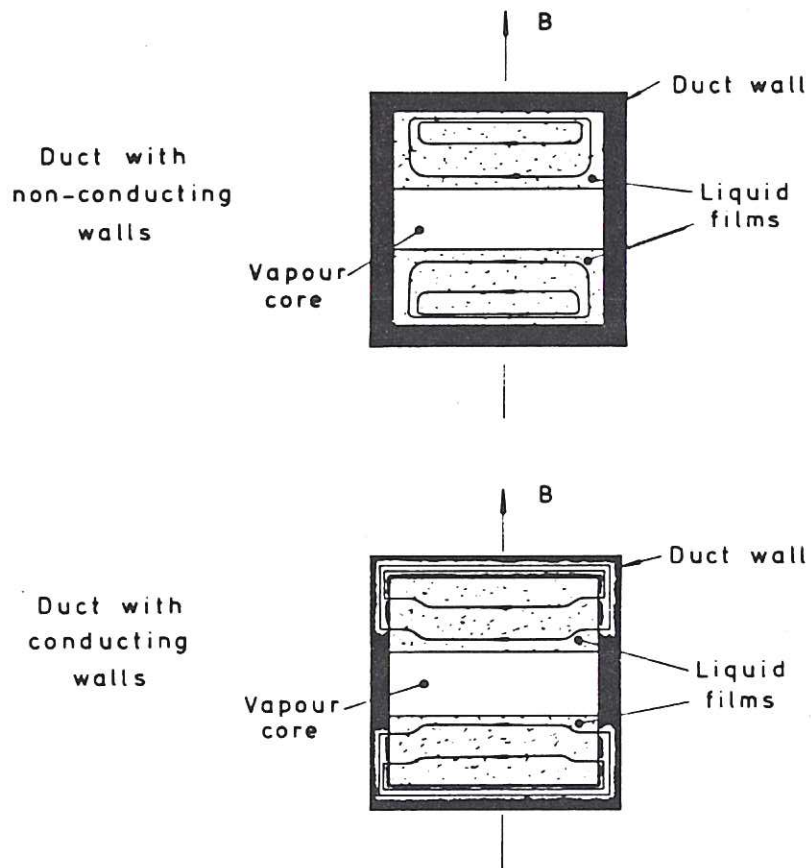


FIG.2. ELECTRIC CURRENT PATHS IN TWO-PHASE FLOW DUE TO A STRONG TRANSVERSE MAGNETIC FIELD. THE VELOCITY IS OUT OF THE PAGE.

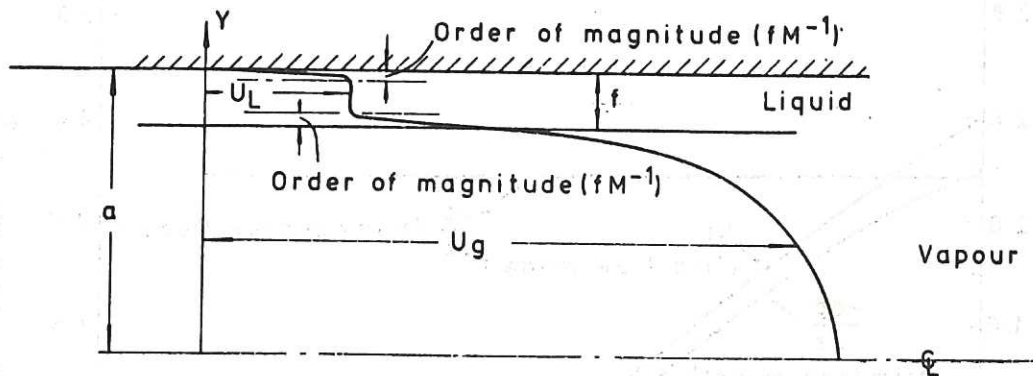


FIG.3. THE VELOCITY PROFILES FOR THE GAS AND LIQUID PHASES.

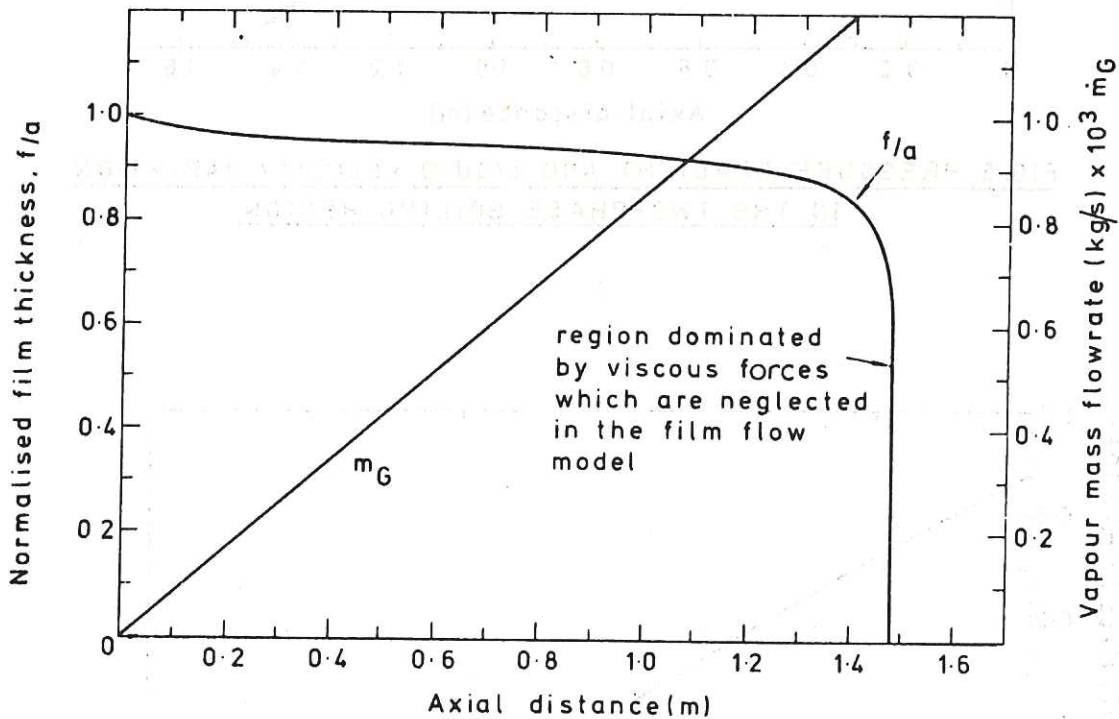


FIG.4. LIQUID FILM THICKNESS AND VAPOUR MASS FLOWRATE VARIATION WITH AXIAL DISTANCE AS COMPUTED BY THE FILM FLOW MODEL.

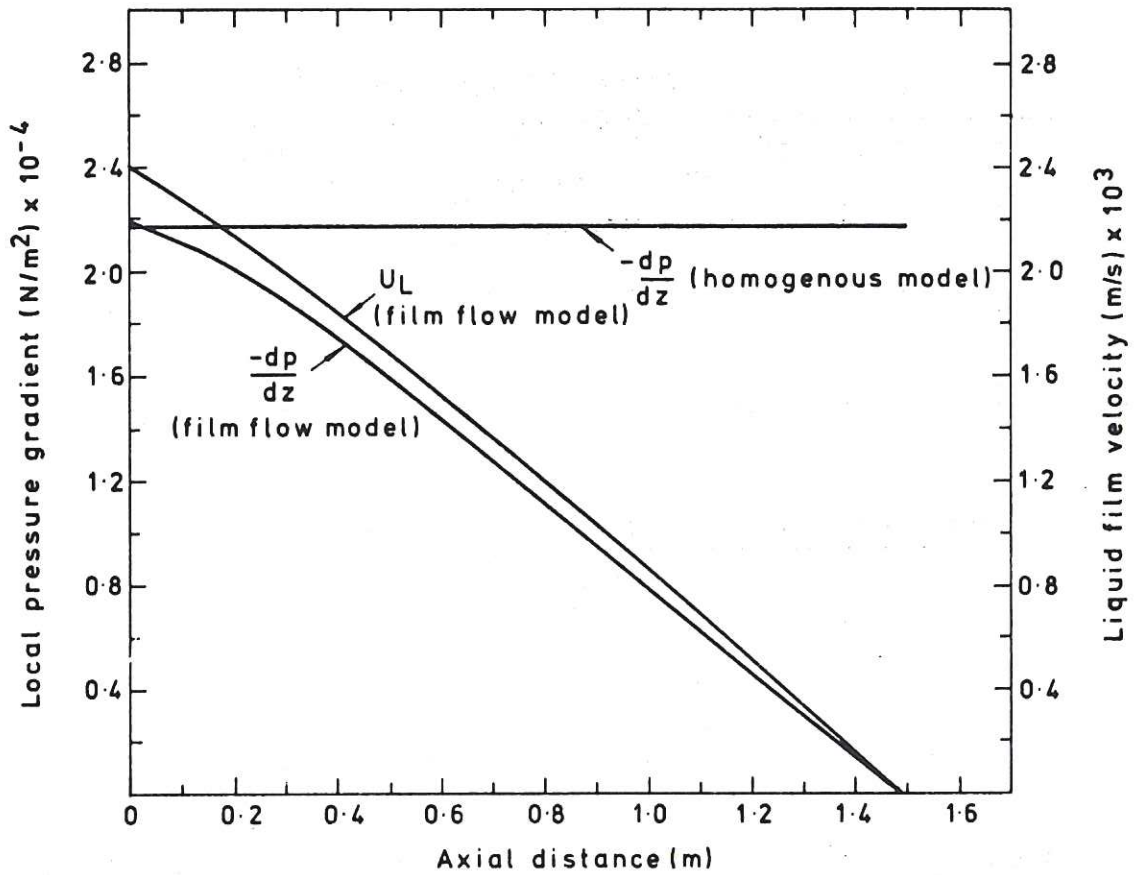


FIG. 5. PRESSURE GRADIENT AND LIQUID VELOCITY VARIATION IN THE TWO-PHASE BOILING REGION.

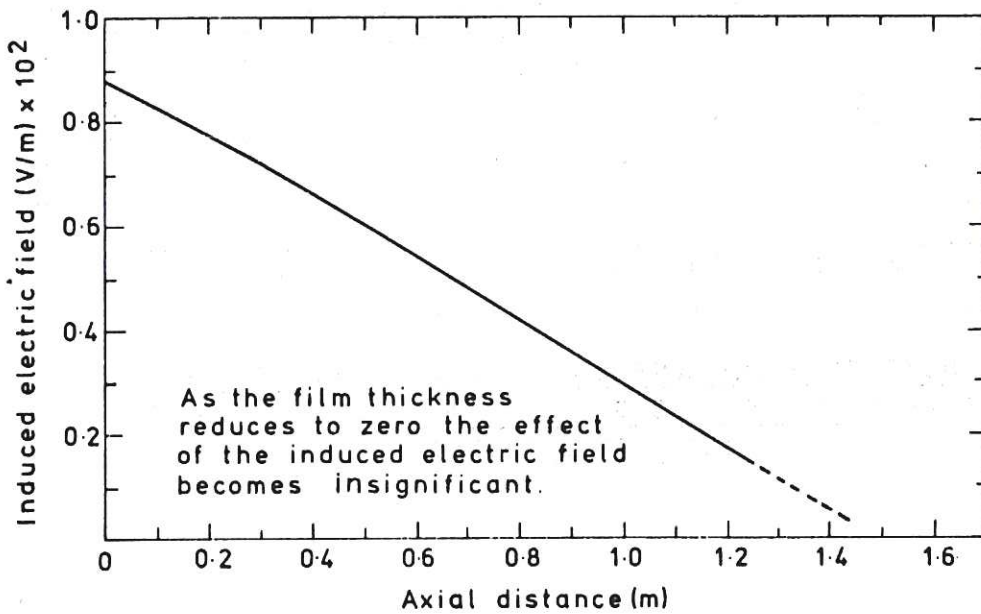


FIG. 6. INDUCED ELECTRIC FIELD VARIATION WITH AXIAL DISTANCE.

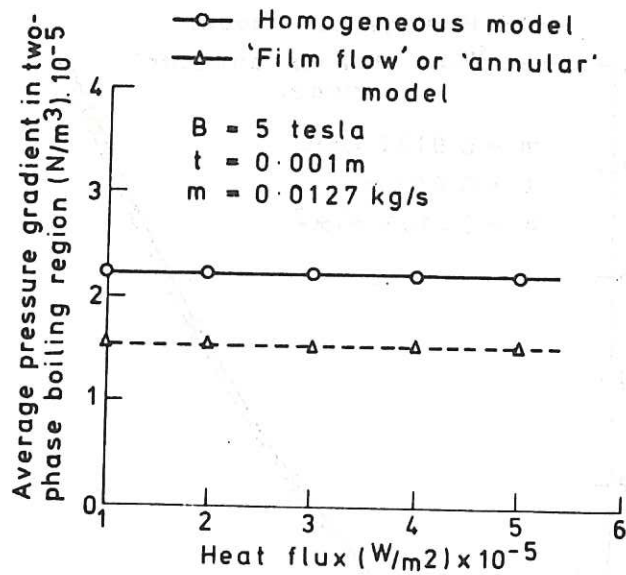


FIG. 7. THE EFFECT OF HEAT FLUX ON PREDICTED AVERAGE PRESSURE GRADIENT IN THE TWO-PHASE BOILING REGION.

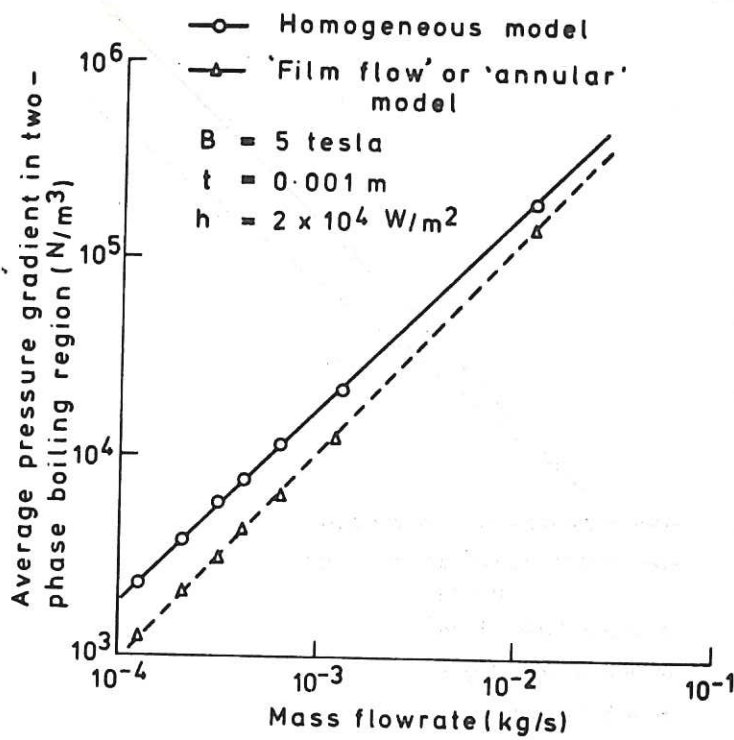


FIG. 8. THE EFFECT OF POTASSIUM MASS FLOWRATE ON PREDICTED AVERAGE PRESSURE GRADIENT IN THE TWO-PHASE BOILING REGION.

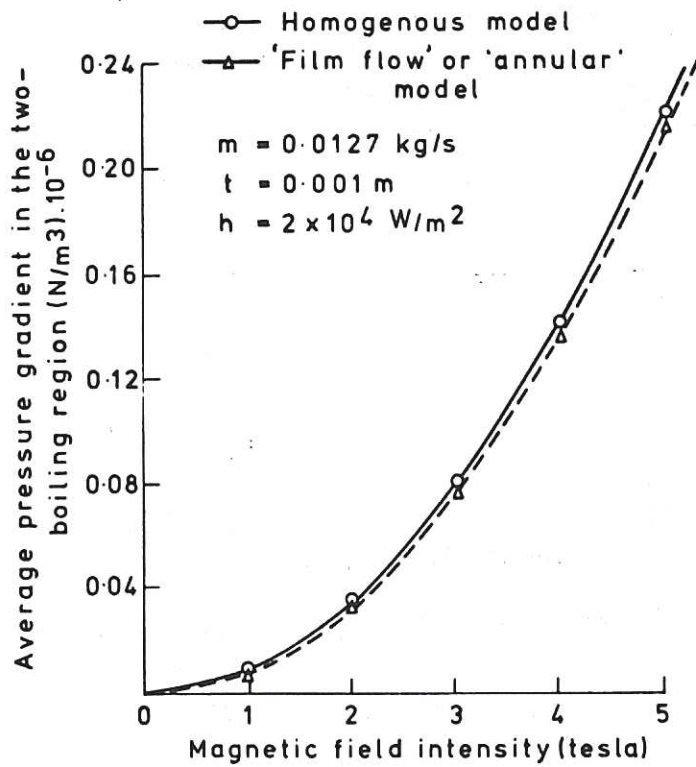


FIG. 9. THE EFFECT OF MAGNETIC FIELD INTENSITY ON THE AVERAGE PRESSURE GRADIENT IN THE TWO-PHASE BOILING REGION.

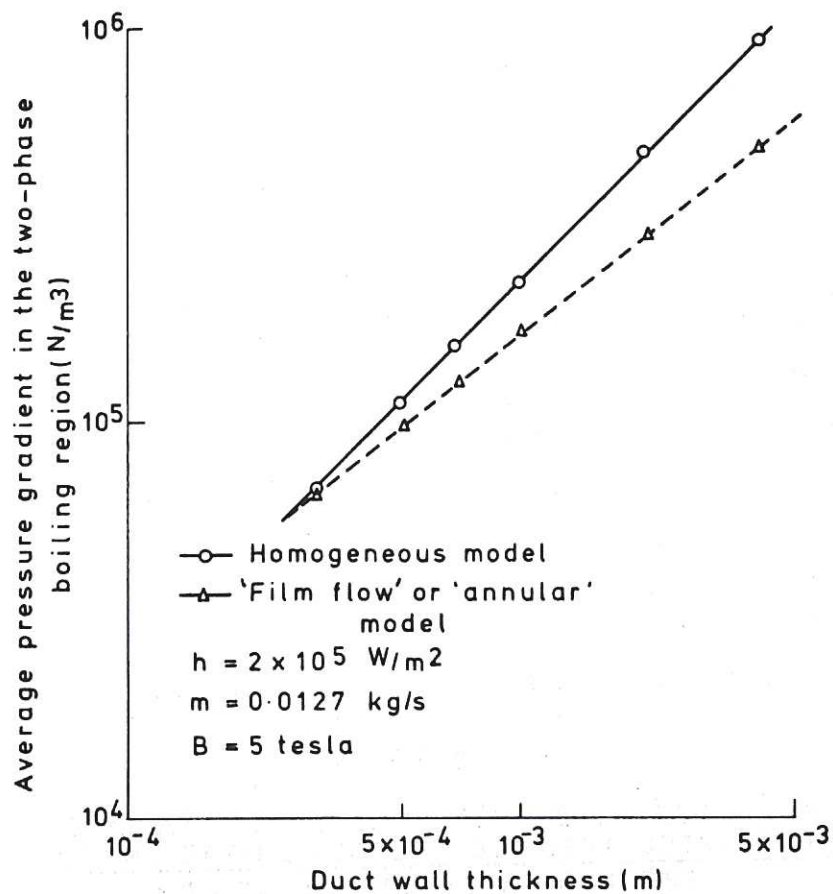


FIG. 10. THE EFFECT OF WALL THICKNESS ON THE AVERAGE PRESSURE GRADIENT IN THE TWO-PHASE BOILING REGION.

The first part of the document discusses the importance of maintaining accurate records of all transactions. It emphasizes that every entry, no matter how small, should be recorded to ensure the integrity of the financial data. This includes not only sales and purchases but also expenses and income. The text suggests that a consistent and thorough record-keeping system is essential for identifying trends and making informed decisions.

In addition, the document highlights the need for regular audits and reconciliations. By comparing the recorded transactions with bank statements and other external records, discrepancies can be identified and corrected promptly. This process helps to prevent errors and fraud, ensuring that the financial statements are reliable and accurate.

The second part of the document focuses on the analysis of the recorded data. It suggests that the information should be organized into clear and concise reports that provide a comprehensive overview of the financial performance. These reports should include key metrics such as profit margins, cash flow, and debt-to-equity ratios. By analyzing these metrics, the business owner can gain valuable insights into the company's financial health and identify areas for improvement.

Finally, the document concludes by emphasizing the importance of transparency and accountability. It encourages the business owner to be open and honest about the financial situation, both internally and with external stakeholders. This transparency is crucial for building trust and ensuring the long-term success of the business.

The following table provides a detailed breakdown of the financial data for the first quarter. It shows the total revenue, the cost of goods sold, and the resulting gross profit. The table also includes a section for operating expenses, which are categorized into fixed and variable costs. This breakdown allows for a more granular analysis of the company's financial performance and helps to identify the most significant areas of expenditure.

Category	Item	Amount
Revenue	Sales	120,000
	Service Fees	80,000
	Licensing	50,000
Cost of Goods Sold	Materials	40,000
	Manufacturing	30,000
Gross Profit	Total	150,000
	Percentage	25%
Operating Expenses	Fixed	20,000
	Variable	15,000
	Depreciation	10,000
	Interest	5,000
Net Income	Total	100,000
	Percentage	16.7%

The data presented in the table indicates that the company has achieved a significant gross profit margin of 25% for the first quarter. However, the operating expenses, particularly the fixed costs, have had a substantial impact on the net income, reducing it to 16.7%. This suggests that while the company is generating revenue, it is also facing high overhead costs that are eroding its profitability.

Based on this analysis, several recommendations can be made to improve the company's financial performance. First, it is essential to review the fixed operating expenses to identify any areas where costs can be reduced or eliminated. This could involve renegotiating contracts with suppliers or optimizing the company's operational processes.

Second, the company should focus on increasing its revenue streams. This could be achieved by expanding the product line, offering new services, or targeting new markets. Additionally, improving the efficiency of the manufacturing process could help to reduce the cost of goods sold, thereby increasing the gross profit margin.

Finally, the company should continue to maintain a high level of transparency and accountability in its financial reporting. Regular audits and reconciliations should be performed to ensure that the financial data is accurate and reliable. This will help to build trust with stakeholders and ensure the long-term success of the business.

